Allometric scaling of faunal-mediated ecosystem functioning: A case study on two bioturbators in contrasting sediments

Fang, X

1 **Allometric scaling of faunal-mediated ecosystem functioning: a case study on two bioturbators in**

2 **contrasting sediments**

3 Xiaoyu Fang[1], Tom Moens[1], Antony Knights[2], Karline Soetaert[3], Carl Van Colen[1*]

4 [1]Marine Biology Research Group, Department of Biology, Ghent University, Krijgslaan 281/S8, 9000

5 Ghent, Belgium

6 [2]School of Biological and Marine Sciences, University of Plymouth, Drake Circus, Plymouth, Devon

7 PL4 8AA, United Kingdom

8 [3]Department of Estuarine and Delta Systems, NIOZ Royal Netherlands Institute for Sea Research and

9 Utrecht University, P.O. Box 140, 4400 AC Yerseke, the Netherlands

10 *corresponding author; carl.vancolen@ugent.be
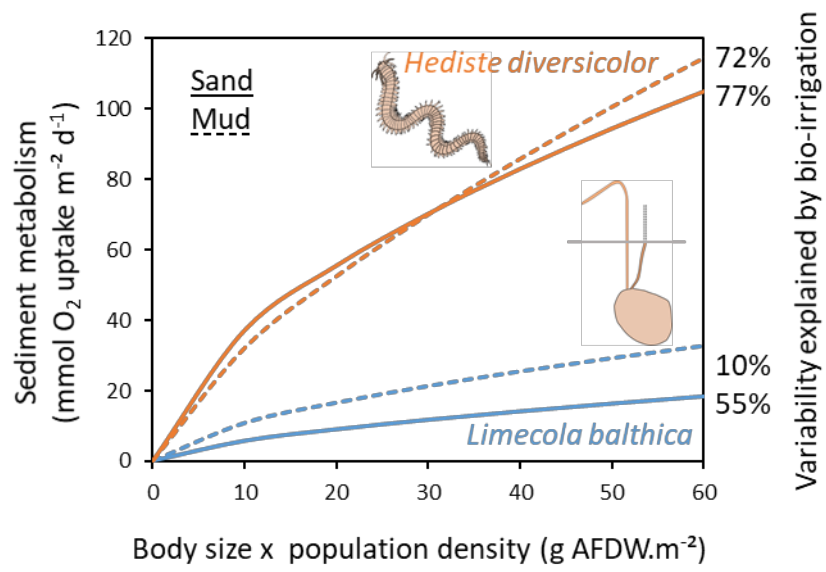
11

12

13

14

15

16

17

18

19

20

21

22

23

24

25

Graphical abstract

41   Highlights

42   • Allometric scaling predicts faunal population effects on seafloor metabolism
43   • Stimulatory effects on sediment metabolism depend on species bioturbation traits
44   • Stimulatory faunal effects on sediment metabolism can vary between sand and mud
45   • Bio-irrigation effects on seafloor metabolism depend on species and sediment type

46

47

48

49

50

51

52

53

54

55

56

57

58

59

60

61

62

63

64

Abstract

Soft-sediment biogeochemistry is influenced by the bioturbation activity of benthic invertebrates. We investigated whether the effect of two macrobenthos bioturbators, *Limecola balthica* and *Hediste diversicolor*, on sediment oxygen uptake can be described by allometric principles of metabolic activity scaling with animal body size and population biomass. Microcosms containing reconstructed populations to control density and individual body size were used to compare bioturbation effects and allometric scaling principles between a sandy and muddy sediment. Both species facilitated oxygen uptake in both sediment types, and a major portion of the variance in sediment metabolism (60-98%) could be explained by the per capita body size and density, and total population biomass. The allometric relationship with the stimulated sediment metabolism was similar in sand and mud for *Hediste* and strongly related to the increasing burrow ventilation rate with population biomass. *Limecola* irrigated less in mud but stimulated sediment metabolism more in mud in comparison to in sand. We discuss how physico-chemical differences between both sediment types, possible changes in activity, and size-dependent irrigation dynamics can explain the variable effects of *Limecola* on sediment metabolism. Overall, we provide empirical evidence that allometric laws can be used to upscale bioturbation effects on ecosystem functioning in marine soft sediments from the individual to the population level.

1. Introduction

Estuaries and coastal marine ecosystems are among the most productive biomes of the world and serve as important life-support ecosystems (Costanza et al., 1997). The biogeochemical cycling of elements that support these productive food webs is influenced by different seabed biota whose activities are directly and indirectly involved in the burial and mineralization of the organic matter settling to the seabed (Kristensen, 2000a; Levinton, 2011; Meysman et al., 2006). Whereas microbial organisms directly govern a variety of biogeochemical reactions, macrobenthos are a group of large (i.e. retained on a 1-mm mesh-sized sieve) sediment-dwelling animals that affect benthic metabolism via aerobic respiration and indirectly via their bioturbation activities. The aerobic metabolism in the sediment community that is stimulated by macrobenthos bioturbation can outweigh the direct O_2 consumption by macrobenthos for respiration purposes (Glud 2008 and references therein). Bioturbation encompasses two main processes: particle reworking and bio-irrigation (Kristensen et al. 2012). Particle reworking results from a series of sediment mixing processes that transport particles and associated living and non-living substances through faunal feeding, defaecation and burrowing activities. Bio-irrigation is the ventilation of burrows with water by the fauna, providing dissolved substances for respiration and particles for feeding. Bioturbation therefore redistributes reduced compounds and aerates the sediment, thereby providing microbial habitats for intensified biogeochemistry (e.g. Mermillod-Blondin et al., 2004; Nielsen et al. 2004; Volkenborn et al. 2012).

Activity of organisms relate to their metabolism that scales with individual body size or mass (Brown et al., 2004; Kooijman 2000). An allometric scaling exponent of approximately 0.75 is evidenced across taxonomic groups, and this 'universal' 3/4 –power law of metabolic rate is often considered as one of the fundamental principles in ecology (West et al. 1997). However, existing taxonomic, environmental and phenotypic (e.g. Barneche et al., 2014; Yvon-Durocher et al., 2012; Clark et al., 2016) variability in metabolic scaling exponents within and among species support ongoing debate (e.g. Glazier, 2015), and other theories that allow for more dynamic body size scaling relationships in function of life stage and environmental conditions have equally found their application in ecology (e.g. Kooijman, 2000). Yet if the bioturbation activity of macrobenthos is proportional to its energetic requirements, the cascading facilitative effect on sediment metabolism can theoretically be assumed to change proportionally to the metabolic rate of the bioturbator. Cozzoli et al. (2018, 2019) support this theory by empirically demonstrating that sediment resuspension can be ascribed to the overall metabolic rate of the bioturbating populations. Furthermore, Wrede et al. (2018) successfully applied a scaling of 0.75 to weigh the effect of body mass on bio-irrigation rates across a range of macrobenthos species populations and communities. The above examples support the idea that (1) an allometric scaling of macrobenthos body size on sediment metabolism can be assumed, and (2) that this metabolic body size

relationship can be scaled as the product of the individual metabolic rate and the population density. However, species metabolic rates depend on abiotic conditions, such as temperature (Clark and Johnston, 1999) and pH (Ong et al. 2017), and variable outcomes of bioturbation effects on sediment metabolism can thus likewise be expected. Indeed, bioturbation activity responds quickly to changes in temperature to support elevated physiological demands at higher temperature (Ouellette et al., 2004), and in general bioturbation rates can respond quickly to changing environmental conditions (Levinton and Kelaher, 2004; Van Colen, Ong et al., 2020, Mestdagh et al. 2020a). Besides inter– and intraspecific variability in stimulatory effects on sediment metabolism related to species biological (e.g. body size) and functional (e.g. sediment reworking mode) traits (Queirós et al. 2013), the local sediment habitat can be important as well. For example, stimulatory effects of macrobenthos on sediment metabolism were shown to be limited in permeable, well-oxygenated sediments as compared to cohesive, organically enriched sediments (Mermillod-Blondin and Rosenberg, 2006). In conclusion, the contribution of macrobenthos to sediment metabolism may vary between species and change considerably over time and across space (Godbold et al., 2011; Needham et al., 2010).

Oxygen is the most favourable electron acceptor in biogeochemical reactions, and the sediment community O_2 consumption (SCOC) is the most widely used measure of aerobic benthic metabolism (Glud, 2008; Thamdrup and Canfield, 2011). SCOC represents a good proxy for the total benthic carbon mineralization rate or sediment metabolism (Canfield et al., 1993) and integrates the re-oxidation of reduced metabolites and the aerobic respiration of benthic organisms. In this study, we quantified the influence of the ragworm *Hediste (*formerly *Nereis) diversicolor* and the Baltic tellin *Limecola (*formerly *Macoma) balthica* (hereafter referred to as *Hediste* and *Limecola*) on the sediment metabolism of an estuarine muddy and sandy sediment. Both species are common in temperate estuaries where they typically constitute a significant part of the macrobenthos biomass (e.g. Ysebaert et al., 2003) and bioturbate the sediment matrix (Fang et al. 2019). Microcosms with various densities and sizes of animals were used to quantify the stimulatory effect of both species on sediment metabolism (measured as SCOC) in both sediment types. We hypothesized that (1) allometric principles of metabolic scaling with population density can be applied to quantify the faunal effects on sediment metabolism; but also that (2) dissimilar porewater solute dynamics related to different bioturbation modalities of both species (see 2.1), and (3) contrasting physico-chemical conditions between sandy and muddy sediments, would affect faunal-mediated sediment metabolism. Finally, we evaluated whether the stimulated sediment metabolism can be explained by the variability in bio-irrigation measured across microcosms.

2. Materials and methods

2.1 Model organisms

Hediste is a highly mobile polychaete that lives in a mucus-lined gallery of semi-permanent U or Y shaped burrows extending 6 to 12 cm into the sediment (Davey, 1994). Muscular movements of the body create currents of oxygen-rich water and suspended food particles into the burrow; active ventilation periods last about 10 minutes and are alternated with 5-minute resting periods (Riisgård 1991; Kristensen, 2001). *Hediste* obtains food from deposit and suspension feeding, as well as via active scavenging and predation on small invertebrates (Scaps 2002 and references therein). The species' sediment reworking and ventilation activities affect other benthos populations, biogeochemistry and sediment erodibility (Hiddink et al., 2002; Kristensen and Mikkelsen, 2003; Widdows et al., 2009). *Limecola* is a facultative surface deposit feeding tellinid bivalve, foraging on microphytobenthos, bacteria and labile organic matter present on the sediment surface or suspended in the water column (Kamermans, 1994; Rossi et al., 2004). The living depth in the sediment depends on the length of the inhalant siphon (Zwarts et al., 1994) that is used to feed and respire on the sediment-water interface. *Limecola* intermittently irrigates the sediment during feeding and respiration via the release of water and solutes through the exhalent siphon just below the sediment surface (Volkenborn et al., 2012), thereby affecting sediment biogeochemistry (Michaud et al., 2006). Resting periods between the irrigation bouts are short (< 2 minutes) and can result in an almost continuous oxygenation in permeable sediments (Volkenborn et al., 2012).

2.2 Sediment and animal collection

Sediments were collected in May 2017 from the Paulina intertidal flat in the polyhaline reach of the Scheldt estuary, SW Netherlands. There are a variety of habitats on this tidal flat, varying from mud to sands almost devoid of silt (Gallucci et al., 2005; Van Colen et al. 2010). A sandy (51°21' 00.2" N, 3° 43' 54.9" E) and a muddy location (51° 20' 57.1" N, 3° 43' 35.4" E) were chosen. The sediment at the sandy location had a higher permeability and oxygen penetration depth but a lower organic carbon content as compared to the muddy location (Table 1). Sediments were collected through coring (inner diameter: 9 cm) and subsequently sectioned into 0-1, 1-2, 2-4, 4-6 cm sediment fractions before macrobenthos and large particles were removed through wet sieving (1 mm mesh size). Each sediment section was incubated at 15°C in aerated seawater collected from the sampling location and allowed to settle prior to reconstruction of the vertical sediment matrix in a rectangular polypropylene box (19.4×29.4×15 cm). Therefore, the 2-4 cm layer was put on top of the deepest layer (4-6 cm) followed by the subsequent deposits of the 1-2 cm and 0-1 cm sediment layers. For each sampling location, two boxes with

193 reconstructed sediment without macrobenthos were acclimated in aerated seawater at 15°C for 4-5
194 weeks before the start of the experiments to maximize stabilisation of the sediment matrix and
195 restoration of biogeochemical gradients before usage in the microcosms (see 2.3).

196 *Limecola* and *Hediste* are ubiquitous and abundant in the polyhaline reach of the Scheldt estuary,
197 occupying both muddy and sandy sediments. In the polyhaline zone of the Scheldt estuary, mean
198 density of *Hediste* is 466 ind. m^{-2} with maxima up to 3928 ind.m^{-2} (corresponding to 13.7 g ash-free dry
199 weight (AFDW) m^{-2}), while *Limecola* attains a mean density of 855 ind. m^{-2} with a maximal density up to
200 5217 ind. m^{-2} (corresponding to 15.9 g. AFDW m^{-2}; after Ysebaert et al., 1998). Individuals of *Hediste* and
201 *Limecola* were collected on 15th June 2017 and left to acclimatize in the natural sediments at 15°C in
202 containers with aerated seawater collected from the sampling location (salinity = 20) until the start of
203 the experiments, which begun within two weeks after collection from the field.

2.3 Experimental design

205 To provide mechanistic insight into the relationship between aerobic sediment metabolism, individual
206 body size, population density, and sediment type, we experimentally tested single-species treatments
207 spanning a broad range of natural body sizes and densities in a muddy and sandy sediment. For each
208 sediment type × species combination, the total sediment O_2 consumption and bio-irrigation were
209 measured in plexiglass cylindrical microcosms (height 12.2 cm, inner diameter 3.6 cm) collected through
210 coring from the boxes with macrobenthos-free sediment (depth 6 cm) and overtopped with *in situ*
211 collected 1-mm sieved seawater. Each series included in total eleven microcosms; one without
212 macrobenthos and ten with combinations of variable densities and a gradient of similarly sized
213 individuals per treatment, yielding a natural density and biomass range for both species (Table 2a, b).
214 The microcosm without macrobenthos was included to distinguish the faunal stimulatory effect by
215 *Hediste* and *Limecola* from the single contribution of microbes and meiofauna activities. The
216 microcosms were aerated, and the organisms were carefully put on top of the sediment and left to
217 acclimatize and burrow overnight into the sediment.

218 The O_2 consumption in the water column was measured using O_2 optodes (Pyroscience OXROB10)
219 connected to a FireSting O_2 meter (FSO$_2$-4). After a two-point calibration, each O_2 optode was inserted
220 through a rubber cap keeping the microcosms airtight during O_2 consumption measurements.
221 Microcosms were put on a platform shaker to assure homogenous mixing of O_2 in the water column;
222 the incubation lasted till O_2 concentration had dropped to 60% of the initial concentration. Sediment
223 oxygen consumption was calculated from the decline in dissolved O_2 concentrations over time,
224 considering both the sediment surface and the volume of the overlying water. Macrobenthos-mediated
225 O_2 uptake in the microcosms was calculated by subtracting the O_2 uptake measured in the microcosm

226 without macrobenthos from that experiment. This faunal-mediated O_2 uptake includes both *Hediste* or

227 *Limecola* respiration and stimulation of respiration by bacteria and meiobenthos.

228 Following the SCOC measurements, microcosms were aerated and left to acclimatise overnight. The

229 following day, seawater was replaced by an aerated solution of seawater and uranine (10 µg.L^{-1}

230 $C_{20}H_{10}NaO_5^-$). Subsequently, 1.5-ml water samples were taken from the water column by Pasteur

231 pipettes at 0, 2, 4, 22.5, 24 h and the uranine concentrations were measured at 520 nm using a Turner

232 Quantech Digital Fluorometer (FM 109530-33) with 490 nm as the excitation wavelength. Uranine fluxes

233 were estimated from the linear decrease of water column tracer concentration over time and used as a

234 proxy for sediment community irrigation rates (Meysman et al. 2007), after standardization per surface

235 area.

236 Total biomass (g AFDW.m^{-2}) of *Hediste* and *Limecola* individuals from each microcosm was measured at

237 the end of the irrigation measurements by loss on ignition after muffling of dried organisms for 3 h at

238 550°C. Individual body size (mg AFDW) was estimated by dividing the total biomass per treatment by

239 the number of individuals.

2.4 Data analysis

241 Following ecological scaling theory (e.g. Brown et al., 2004), the mediating effect on sediment

242 metabolism performed by a homogeneous population can be expressed as a power function $Y=aM^bA$

243 [1], where Y is the faunal-mediated O_2 uptake, and M and A are the respective individual body size (mg

244 AFDW) and the density of the examined animals; a is the coefficient quantified in the model, and b is

245 the allometric exponent relating body size to individual activity. Equation [1] can be modified to include

246 population biomass W: $Y = cW^d$ [2], where c is the quantified coefficient and d is the biomass-dependent

247 scaling exponent.

248 Analysis of covariance (ANCOVA) was conducted to compare the faunal-mediated O_2 uptake between

249 sediment types while controlling for the biomass range across treatments. Biomass of *Hediste* and

250 *Limecola* were normalized using log transformation in all experiments to meet assumptions of the

251 homogeneity of regression slopes and the homogeneity of variances. Finally, simple linear regression

252 was used to determine to what extent the variance of faunal-mediated O_2 uptake can be explained by

253 bio-irrigation of the sediment community. P-P plots and scatterplots of residuals against the explanatory

254 variable revealed that no further data transformation was needed to meet assumptions of normality

255 and homoscedasticity. The level for statistical significance was set at 0.05 in all analyses.

256

3. Results and discussion

Sediment O_2 consumption by microbial and meiobenthos communities alone was 8.8 ± 2.3 SD mmol m^{-2} d^{-1} (n = 2) and 1.9 ± 0.3 SD mmol m^{-2} d^{-1} (n = 2) in muddy and sandy sediments, respectively, which was marginal in comparison to the SCOC rates in microcosms with macrobenthos (Figure 1a,b). *In situ* measurements and experimental data show that faunal respiration typically accounts for 10-40% of the faunal-mediated O_2 consumption (e.g. Glud et al. 2003; Glud, 2008; Dunn et al. 2009; Kristensen 1985); the remaining portion is than ascribed to the stimulated microbial activity related to the bioturbation activity, i.e. particle mixing and bio-irrigation. Bio-irrigation rates by meiobenthos alone were 12.7 ± 0.2 SD L.m^{-2}.d^{-1} (n = 2) and 2.7 ± 1.0 SD L.m^{-2}.d^{-1} (n = 2) in muddy and sandy sediments, respectively. The additional irrigation by *Hediste* and *Limecola* explained a significant portion of the faunal-mediated O_2 uptake (R² = 0.55 − 0.77, p < 0.01) in all experimental series, except for the stimulated sediment metabolism by *Limecola* in the muddy sediments (R² = 0.10, p = 0.37) (Figure 2a,b). Irrigation rates for *Limecola* across body size × density combinations in the muddy sediments were generally lower as compared to the sandy sediments, and in the same order of magnitude as for irrigation by meiobenthos alone. Irrigation by *Limecola* mainly occurs when the water that is inhaled during feeding is injected into the sediment via the exhalent siphon (Volkenborn et al. 2012). It is therefore likely that *Limecola* individuals reduced feeding (and irrigating) events in organically enriched muddy sediment as compared to the food poor sandy sediment. We furthermore hypothesize that limited porewater advection (e.g. Hedman et al., 2011) reduced the relative importance of bio-irrigation for organic matter mineralisation in the muddy sediment. Despite the limited contribution of bio-irrigation, the *Limecola*-mediated sediment O_2 uptake was significantly higher in muddy as compared to sandy sediments when considering the population biomass variation across treatments (0.9 ± 0.3 mmol O_2 gAFDW^{-1} d^{-1} and 0.4 ± 0.2 mmol O_2 gAFDW^{-1} d^{-1} in muddy and sandy sediments respectively; ANCOVA: Sediment type p < 0.001, Table 3), which might be explained by the higher availability of reduced metabolites in muddy sediments (e.g. Kristensen et al. 2000b). In comparison, the stimulated O_2 uptake by *Hediste* was higher than that of *Limecola* (2.6 ± 1.8 mmol O_2 gAFDW^{-1} d^{-1} and 2.5 ± 0.9 mmol O_2 gAFDW^{-1} d^{-1} in muddy and sandy sediments respectively), but did not vary between sediment types (ANCOVA: Sediment type p = 0.678, Table 3). The stronger enhancement of aerobic sediment metabolism by gallery-burrowing polychaetes in comparison to biodiffusing bivalves corroborates earlier findings by Michaud et al. (2005) for populations from the St. Lawrence estuary. The periodic ventilation of the deep *Hediste* gallery burrow system (Kristensen, 1981; Pischedda et al., 2012) in comparison to the more continuous diffusion that is limited to the surface sediment by *Limecola* (Volkenborn et al. 2012) can explain this species effect. The creation of the gallery burrow system expands the sediment – seawater interface for solute exchange several-fold, and redox oscillations such as those generated through periodic

ventilation activities are known to strongly stimulate microbial organic matter mineralisation (e.g. Aller, 1994). Indeed, *Hediste* was detected as a key irrigator in intertidal sediments along the Scheldt estuary (Fang et al., 2019), where irrigation contributed significantly to the sediment metabolism (Mestdagh et al., 2020b). The fact that oxygen dynamics generated by *Hediste* irrigation are restricted to the burrow lumen and a few mm in the burrow wall (Pischedda et al. 2012; Nielsen et al. 2004) may explain why cascading effects on sediment metabolism did not differ between sediments despite differences in sediment permeability and organic matter content (Table 1). However, longer incubations could have yielded different results because sediment type can affect body condition, which in turn influences burrowing depth (Esselink and Zwarts, 1989). Furthermore, the increasing depth and complexity of burrow structures with incubation time is known to increase oxygen uptake in marine sediments (e.g. Michaud et al. 2005, Gilbert et al. 1994, 1995).

For both species the faunal-mediated O_2 consumption followed an allometric power law as a function of body size and density in both sediment types, supporting the metabolic theory of ecology (Brown et al. 2004) (Table 4). For both sediment types, the model based on population biomass explained the variability in *Hediste*-mediated O_2 uptake better (adjusted $R^2 > 0.95$) as compared to the allometric model that considers the scaled body size component and population density (adjusted $R^2 < 0.85$). This suggests that for this species, non-linear density effects on solute exchange may exist, such as e.g. space limitation for burrow construction (Aller, 2004). The biomass size scaling exponents for *Hediste* (0.58 - 0.71, Table 4) are in accordance with the quantified relationships between oxygen consumption and body weight in eight marine polychaetes (0.61-0.69; Shumway, 1979), further supporting the metabolic basis of the stimulatory effect on sediment metabolism. In contrast, the predictive power of both allometric models for *Limecola* was similar, suggesting that density-dependent interference amongst *Limecola* individuals is less important than for a more mobile species like *Hediste*. On the other hand, the stimulated sediment metabolism in function of body size and density or population biomass of *Limecola* was clearly better explained for the muddy (adjusted $R^2 > 0.88$) than for the sandy sediments (adjusted $R^2 < 0.64$)(Table 4). This may result from constraints on depth distribution set by body size, and from environmental constraints on how metabolic activity and bioturbation affect sediment metabolism. That is, as shorter siphon lengths in small individuals decrease burrowing depth (Zwarts et al., 1994), the shallow advective irrigation flows generated by smaller individuals might not have contributed importantly to sediment metabolism in the sandy sediment that is characterized by a deeper diffusive oxygen penetration (Table 1).

4. Conclusion

We demonstrate that ecological scaling laws based on body size allometry can be applied to predict sediment metabolism based on the bioturbation effect of two macrobenthos species with different sediment particle reworking and ventilation traits. Similarly, Cozzoli et al. (2019) found that allometric principles of metabolic activity scaling and population size explained the bioturbation impact of different macrobenthos species on sediment resuspension. Allometric laws based on body size and population density can thus be used to upscale species effects on ecosystem functioning in marine soft sediments from the individual to the population level. However, this work also corroborates earlier findings that sediment texture can modify bioturbation effects on ecosystem functioning (e.g. Li et al., 2017; Joenssuu et al., 2018; Van Colen et al., 2013), depending on how species interact with their environment. This demonstrates that insights into how environmental conditions can modify organism activity and metabolism (e.g. Halsey et al. 2015; Cornwell et al. 2020), and the cascading effects this may have on ecosystem functioning, are needed before allometric extrapolations can be applied to larger spatial (e.g. the entire estuary) and temporal scales, encompassing e.g. gradients in salinity, temperature and sediment composition.

5. Acknowledgments

6. References

Aller, R.C., 1994. Bioturbation and Remineralization of Sedimentary Organic-Matter - Effects of Redox Oscillation. Chem Geol 114, 331-345.

Aller, R.C., 2004. Conceptual models of early diagenetic processes: The muddy seafloor as an unsteady, batch reactor. J Mar Res 62, 815-835.

Barneche, D.R., Allen, A.P., 2015. Embracing general theory and taxon-level idiosyncrasies to explain nutrient recycling. P Natl Acad Sci USA 112, 6248-6249.

Brown, J.H., Gillooly, J.F., Allen, A.P., Savage, V.M., West, G.B., 2004. Toward a metabolic theory of ecology. Ecology 85, 1771-1789.

355 Canfield, D.E., Jorgensen, B.B., Fossing, H., Glud, R., Gundersen, J., Ramsing, N.B., Thamdrup, B., Hansen,
356   J.W., Nielsen, L.P., Hall, P.O.J., 1993. Pathways of Organic-Carbon Oxidation in 3 Continental-
357   Margin Sediments. Mar Geol 113, 27-40.

358 Clark, R.M., Zera, A.J., Behmer, S.T., 2016. Metabolic rate is canalized in the face of variable life history
359   and nutritional environment. Funct Ecol 30, 922-931.

360 Clarke, A., Johnston, N.M., 1999. Scaling of metabolic rate with body mass and temperature in teleost
361   fish. J Anim Ecol 68, 893-905.

362 Cornwell, T.O., McCarthy, I.D., Biro, P.A., 2020. Integration of physiology, behaviour and life history
363   traits: personality and pace of life in a marine gastropod. Anim Behav 163, 155-162.

364 Costanza, R., dArge, R., deGroot, R., Farber, S., Grasso, M., Hannon, B., Limburg, K., Naeem, S., ONeill,
365   R.V., Paruelo, J., Raskin, R.G., Sutton, P., vandenBelt, M., 1997. The value of the world's
366   ecosystem services and natural capital. Nature 387, 253-260.

367 Cozzoli, F., Bouma, T.J., Ottolander, P., Lluch, M.S., Ysebaert, T., Herman, P.M.J., 2018. The combined
368   influence of body size and density on cohesive sediment resuspension by bioturbators. Sci Rep-
369   Uk 8.

370 Cozzoli, F., Gjoni, V., Del Pasqua, M., Hu, Z., Ysebaert, T., Herman, P.M.J., Bouma, T.J., 2019. A process
371   based model of cohesive sediment resuspension under bioturbators' influence. Sci Total Environ
372   670, 18-30.

373 Davey, J.T., 1994. The Architecture of the Burrow of Nereis-Diversicolor and Its Quantification in Relation
374   to Sediment-Water Exchange. J Exp Mar Biol Ecol 179, 115-129.

375 Dunn, R.J.K., Welsh, D.T., Jordan, M.A., Teasdale, P.R., Lemckert, C.J., 2009. Influence of natural
376   amphipod (Victoriopisa australiensis) (Chilton, 1923) population densities on benthic
377   metabolism, nutrient fluxes, denitrification and DNRA in sub-tropical estuarine sediment.
378   Hydrobiologia 628, 95-109.

379 Eggleston, J., Rojstaczer, S., 1998. Inferring spatial correlation of hydraulic conductivity from sediment
380   cores and outcrops. Geophys Res Lett 25, 2321-2324.

381 Esselink, P., Zwarts, L., 1989. Seasonal Trend in Burrow Depth and Tidal Variation in Feeding-Activity of
382   Nereis-Diversicolor. Mar Ecol Prog Ser 56, 243-254.

383 Fang, X.Y., Mestdagh, S., Ysebaert, T., Moens, T., Soetaert, K., Van Colen, C., 2019. Spatio-temporal
384   variation in sediment ecosystem processes and roles of key biota in the Scheldt estuary. Estuar
385   Coast Shelf S 222, 21-31.

386 Gallucci, F., Steyaert, M., Moens, T., 2005. Can field distributions of marine predacious nematodes be
387   explained by sediment constraints on their foraging success? Mar Ecol Prog Ser 304, 167-178.

388 Gilbert, F., Bonin, P., Stora, G., 1995. Effect of Bioturbation on Denitrification in a Marine Sediment from
389   the West Mediterranean Littoral. Hydrobiologia 304, 49-58.

390 Gilbert, F., Rivet, L., Bertrand, J.C., 1994. The in-Vitro Influence of the Burrowing Polychaete Nereis-
391   Diversicolor on the Fate of Petroleum-Hydrocarbons in Marine-Sediments. Chemosphere 29, 1-
392   12.

393 Glazier, D.S., 2015. Is metabolic rate a universal 'pacemaker' for biological processes? Biol Rev 90, 377-
394   407.

395 Glud, R.N., 2008. Oxygen dynamics of marine sediments. Mar Biol Res 4, 243-289.

396 Glud, R.N., Gundersen, J.K., Roy, H., Jorgensen, B.B., 2003. Seasonal dynamics of benthic O-2 uptake in
397   a semienclosed bay: Importance of diffusion and faunal activity. Limnol Oceanogr 48, 1265-
398   1276.

399 Godbold, J.A., Bulling, M.T., Solan, M., 2011. Habitat structure mediates biodiversity effects on
400   ecosystem properties. P Roy Soc B-Biol Sci 278, 2510-2518.

401 Halsey, L.G., Matthews, P.G.D., Rezende, E.L., Chauvaud, L., Robson, A.A., 2015. The interactions
402   between temperature and activity levels in driving metabolic rate: theory, with empirical
403   validation from contrasting ectotherms. Oecologia 177, 1117-1129.

404 Hedman, J.E., Gunnarsson, J.S., Samuelsson, G., Gilbert, F., 2011. Particle reworking and solute transport
405   by the sediment-living polychaetes Marenzelleria neglecta and Hediste diversicolor. J Exp Mar
406   Biol Ecol 407, 294-301.

407 Hiddink, J.G., ter Hofstede, R., Wolff, W.J., 2002. Predation of intertidal infauna on juveniles of the
408   bivalve Macoma balthica. J Sea Res 47, 141-159.

409 Joensuu, M., Pilditch, C.A., Harris, R., Hietanen, S., Pettersson, H., Norkko, A., 2018. Sediment properties,
410   biota, and local habitat structure explain variation in the erodibility of coastal sediments. Limnol
411   Oceanogr 63, 173-186.

412 Kamermans, P., 1994. Similarity in Food Source and Timing of Feeding in Deposit-Feeding and
413   Suspension-Feeding Bivalves. Mar Ecol Prog Ser 104, 63-75.

414 Kooijman, S., 2000. Dynamic Energy and Mass Budgets in Biological Systems. Cambridge University
415   Press, Cambridge.

416 Kristensen, E., 1981. Direct Measurement of Ventilation and Oxygen-Uptake in 3 Species of Tubicolous
417   Polychaetes (Nereis Spp). J Comp Physiol 145, 45-50.

418 Kristensen, E., 2000a. Organic matter diagenesis at the oxic/anoxic interface in coastal marine
419   sediments, with emphasis on the role of burrowing animals. Hydrobiologia 426, 1-24.

420 Kristensen, E., 2001. Impact of polychaetes (Nereis and Arenicola) on sediment biogeochemistry in
421   coastal areas: Past, present, and future developments. Abstr Pap Am Chem S 221, U538-U538.

422 Kristensen, E., Bodenbender, J., Jensen, M.H., Rennenberg, HK, Jensen, K.M., 2000b. Sulfur cycling of
423   intertidal Wadden Sea sediments (Konigshafen, Island of Sylt, Germany): sulfate reduction and
424   sulfur gas emission. J Sea Res 43, 93-104.

425   Kristensen, E., Jensen, M.H., Andersen, T.K., 1985. The Impact of Polychaete (Nereis-Virens Sars)
426   Burrows on Nitrification and Nitrate Reduction in Estuarine Sediments. J Exp Mar Biol Ecol 85,
427   75-91.

428   Kristensen, E., Mikkelsen, O.L., 2003. Impact of the burrow-dwelling polychaete Nereis diversicolor on
429   the degradation of fresh and aged macroalgal detritus in a coastal marine sediment. Mar Ecol
430   Prog Ser 265, 141-153.

431   Kristensen, E., Penha-Lopes, G., Delefosse, M., Valdemarsen, T., Quintana, C.O., Banta, G.T., 2012. What
432   is bioturbation? The need for a precise definition for fauna in aquatic sciences. Mar Ecol Prog
433   Ser 446, 285-302.

434   Levinton, J., 2011. Bioturbators as Ecosystem Engineers: Control of the Sediment Fabric, Inter-Individual
435   Interactions, and Material Fluxes, in: Linking Species & Ecosystems. pp. 29–36.

436   Li, B.Q., Cozzoli, F., Soissons, L.M., Bouma, T.J., Chen, L.L., 2017. Effects of bioturbation on the erodibility
437   of cohesive versus non-cohesive sediments along a current-velocity gradient: A case study on
438   cockles. J Exp Mar Biol Ecol 496, 84-90.

439   Mermillod-Blondin, F., Rosenberg, R., 2006. Ecosystem engineering: the impact of bioturbation on
440   biogeochemical processes in marine and freshwater benthic habitats. Aquat Sci 68, 434-442.

441   Mermillod-Blondin, F., Rosenberg, R., Francois-Carcaillet, F., Norling, K., Mauclaire, L., 2004. Influence
442   of bioturbation by three benthic infaunal species on microbial communities and biogeochemical
443   processes in marine sediment. Aquat Microb Ecol 36, 271-284.

444   Mestdagh, S., Fang, X.Y., Soetaert, K., Ysebaert, T., Moens, T., Van Colen, C., 2020. Seasonal variability
445   in ecosystem functioning across estuarine gradients: The role of sediment communities and
446   ecosystem processes. Mar Environ Res 162.

447   Mestdagh, S., Ysebaert, T., Moens, T., Van Colen, C., 2020. Dredging-induced turbid plumes affect bio-
448   irrigation and biogeochemistry in sediments inhabited by Lanice conchilega (Pallas, 1766). Ices
449   J Mar Sci 77, 1219-1226.

450   Meysman, F.J.R., Galaktionov, O.S., Cook, P.L.M., Janssen, F., Huettel, M., Middelburg, J.J., 2007.
451   Quantifying biologically and physically induced flow and tracer dynamics in permeable
452   sediments. Biogeosciences 4, 627-646.

453   Meysman, F.J.R., Middelburg, J.J., Heip, C.H.R., 2006. Bioturbation: a fresh look at Darwin's last idea.
454   Trends Ecol Evol 21, 688-695.

455   Michaud, E., Desrosiers, G., Mermillod-Blondin, F., Sundby, B., Stora, G., 2005. The functional group
456   approach to bioturbation: The effects of biodiffusers and gallery-diffusers of the Macoma
457   balthica community on sediment oxygen uptake. J Exp Mar Biol Ecol 326, 77-88.

458   Michaud, E., Desrosiers, G., Mermillod-Blondin, F., Sundby, B., Stora, G., 2006. The functional group
459   approach to bioturbation: II. The effects of the Macoma balthica community on fluxes of

460   nutrients and dissolved organic carbon across the sediment-water interface. J Exp Mar Biol Ecol
461   337, 178-189.

462 Needham, H.R., Pilditch, C.A., Lohrer, A.M., Thrush, S.F., 2010. Habitat dependence in the functional
463   traits of Austrohelice crassa, a key bioturbating species. Mar Ecol Prog Ser 414, 179-193.

464 Nielsen, O.I., Gribsholt, B., Kristensen, E., Revsbech, N.P., 2004. Microscale distribution of oxygen and
465   nitrate in sediment inhabited by Nereis diversicolor: spatial patterns and estimated reaction
466   rates. Aquat Microb Ecol 34, 23-32.

467 Ong, E.Z., Briffa, M., Moens, T., Van Colen, C., 2017. Physiological responses to ocean acidification and
468   warming synergistically reduce condition of the common cockle Cerastoderma edule. Mar
469   Environ Res 130, 38-47.

470 Ouellette, D., Desrosiers, G., Gagne, J.P., Gilbert, F., Poggiale, J.C., Blier, P.U., Stora, G., 2004. Effects of
471   temperature on in vitro sediment reworking processes by a gallery biodiffusor, the polychaete
472   Neanthes virens. Mar Ecol Prog Ser 266, 185-193.

473 Pischedda, L., Cuny, P., Esteves, J.L., Poggiale, J.C., Gilbert, F., 2012. Spatial oxygen heterogeneity in a
474   Hediste diversicolor irrigated burrow. Hydrobiologia 680, 109-124.

475 Queiros, A.M., Birchenough, S.N.R., Bremner, J., Godbold, J.A., Parker, R.E., Romero-Ramirez, A., Reiss,
476   H., Solan, M., Somerfield, P.J., Van Colen, C., Van Hoey, G., Widdicombe, S., 2013. A bioturbation
477   classification of European marine infaunal invertebrates. Ecol Evol 3, 3958-3985.

478 Riisgard, H.U., 1991. Suspension Feeding in the Polychaete Nereis-Diversicolor. Mar Ecol Prog Ser 70,
479   29-37.

480 Rossi, F., Herman, P.M.J., Middelburg, J.J., 2004. Interspecific and intraspecific variation of delta C-13
481   and delta N-15 in deposit- and suspension-feeding bivalves (Macoma balthica and
482   Cerastoderma edule): Evidence of ontogenetic changes in feeding mode of Macoma balthica.
483   Limnol Oceanogr 49, 408-414.

484 Scaps, P., 2002. A review of the biology, ecology and potential use of the common ragworm Hediste
485   diversicolor (OF Muller) (Annelida : Polychaeta). Hydrobiologia 470, 203-218.

486 Shumway, S.E., 1979. Effects of Body Size, Oxygen-Tension and Mode of Life on the Oxygen-Uptake
487   Rates of Polychaetes. Comp Biochem Phys A 64, 273-278.

488 Thamdrup, B., Canfield, D.E., 2011. Benthic Respiration in Aquatic Sediments, in: Methods in Ecosystem
489   Science. pp. 86–103.

490 Van Colen, C., De Backer, A., Meulepas, G., van der Wal, D., Vincx, M., Degraer, S., Ysebaert, T., 2010.
491   Diversity, trait displacements and shifts in assemblage structure of tidal flat deposit feeders
492   along a gradient of hydrodynamic stress. Mar Ecol Prog Ser 406, 79-89.

493   Van Colen, C., Ong, E.Z., Briffa, M., Wethey, D.S., Abatih, E., Moens, T., Woodin, S.A., 2020. Clam feeding
494   plasticity reduces herbivore vulnerability to ocean warming and acidification. Nat Clim Change
495   10, 162-+.

496   Van Colen, C., Thrush, S.F., Vincx, M., Ysebaert, T., 2013. Conditional Responses of Benthic Communities
497   to Interference from an Intertidal Bivalve. Plos One 8.

498   Volkenborn, N., Meile, C., Polerecky, L., Pilditch, C.A., Norkko, A., Norkko, J., Hewitt, J.E., Thrush, S.F.,
499   Wethey, D.S., Woodin, S.A., 2012. Intermittent bioirrigation and oxygen dynamics in permeable
500   sediments: An experimental and modeling study of three tellinid bivalves. J Mar Res 70, 794-
501   823.

502   West, G.B., Brown, J.H., Enquist, B.J., 1997. A general model for the origin of allometric scaling laws in
503   biology. Science 276, 122-126.

504   Widdows, J., Brinsley, M.D., Pope, N.D., 2009. Effect of Nereis diversicolor density on the erodability of
505   estuarine sediment. Mar Ecol Prog Ser 378, 135-143.

506   Wrede, A., Beermann, J., Dannheim, J., Gutow, L., Brey, T., 2018. Organism functional traits and
507   ecosystem supporting services A novel approach to predict bioirrigation. Ecol Indic 91, 737-743.

508   Ysebaert, T., Herman, P.M.J., Meire, P., Craeymeersch, J., Verbeek, H., Heip, C.H.R., 2003. Large-scale
509   spatial patterns in estuaries: estuarine macrobenthic communities in the Schelde estuary, NW
510   Europe. Estuar Coast Shelf S 57, 335-355.

511   Ysebaert, T., Meire, P., Coosen, J., Essink, K., 1998. Zonation of intertidal macrobenthos in teh estuaries
512   of Schelde and Ems. Aquat. Ecol. 32, 53-71.

513   Yvon-Durocher, G., Caffrey, J.M., Cescatti, A., Dossena, M., del Giorgio, P., Gasol, J.M., Montoya, J.M.,
514   Pumpanen, J., Staehr, P.A., Trimmer, M., Woodward, G., Allen, A.P., 2012. Reconciling the
515   temperature dependence of respiration across timescales and ecosystem types. Nature 487,
516   472-476.

517   Zwarts, L., Blomert, A.M., Spaak, P., Devries, B., 1994. Feeding Radius, Burying Depth and Siphon Size of
518   Macoma-Balthica and Scrobicularia-Plana. J Exp Mar Biol Ecol 183, 193-212.

519

520

521

522

523

524

Tables

526 *Table 1*. Physico-chemical sediment characteristics for the two sampling locations: median grain size (in

527 μm), mud content (in % < 63 μm), total organic carbon (in %), permeability (in m^2) and oxygen

528 penetration depth (in mm). Data were derived from a seasonal survey in the Scheldt estuary in 2015-

529 2016 (Mestdagh et al. 2020b). All values are means ± standard deviations for characteristics obtained

530 in September 2015, December 2015, March 2016, and June 2016. The total organic carbon (TOC) (FLASH

531 2000 NC Analyzer, Thermo Scientific, Wilmington, DE, United States), sediment grain size and mud

532 content (Mastersizer 2000 particle analyser, Malvern Panalytical, Malvern, United Kingdom) were

533 analysed by homogenising a 10 cm deep sample. Permeability was calculated based on Eggleston and

534 Rojstaczer (1998): $KH = 1.1019 \times 103\ m^{-2}\ s * d_{10}^2 * v$, where KH is the permeability (in m^2), d_{10} is the first

535 decile of the grain size distribution (in m), and v is kinematic viscosity (in $m^2\ s^{-1}$) calculated from water

536 temperature and salinity. Oxygen penetration depths were derived from the vertical oxygen profiles

537 using Unisense oxygen microsensors (type OX100) in vertical increments of 250 μm.

538 *Table 2*: Overview of macrofaunal density (Ind.m^{-2}), biomass (g AFDW.m^{-2}) and individual body size (mg

539 AFDW ind^{-1}) in the different treatments. Several combinations of densities and individual body sizes of

540 the target organisms (a) *H. diversicolor* and (b) *L. balthica* were tested according to their natural density

541 range in sandy and muddy sediments in the polyhaline zone of the Scheldt estuary.

542 *Table 3*: ANCOVA results in species subsets: (a) *H. diversicolor* and (b) *L. balthica*. Faunal-mediated O_2

543 uptake is the dependent variable, sediment type is the factor, and biomass is the covariate. Once the

544 significant effect of sediment type was found in the *L. balthica* dataset, the estimated marginal means

545 were analysed.

546 *Table 4*: Summary of allometric models to predict faunal-mediated O_2 uptake (mmol m^{-2} d^{-1}).

547

548

549

550

551

552

553

555   *Table 1*

Property	Sandy	Muddy
Median grain size (µm)	226 ± 3	46 ± 1
Mud content (%)	3,7 ± 1,2	64,8 ± 1,7
TOC (%)	0,2 ± 0,1	1,2 ± 0,1
Permeability (m^2)	$8,17 \ 10^{-11} \pm 1,1 \ 10^{-10}$	$7,17 \ 10^{-14} \pm 1,9 \ 10^{-14}$
Oxygen penetration depth (mm)	7,7 ± 3,2	3,9 ± 0,4

574 *Table 2*

(a) *Hediste diversicolor*	Sandy			Muddy		
Treatment	Density	Biomass	Body size	Density	Biomass	Body size
1	0	0	0	0	0	0
2	943	7.6	8.1	943	2.7	2.8
3	943	28.5	30.2	943	14.6	15.5
4	943	43.1	45.7	943	45.4	48.1
5	1887	17.3	9.2	1887	27.8	14.7
6	1887	3.2	1.7	1887	21.7	11.5
7	2830	105.6	37.3	2830	71.3	25.2
8	3774	114.2	30.3	2830	46.7	16.5
9	4717	61.5	13.0	3774	99.3	26.3
10	4717	42.4	9.0	3774	43.1	11.4
11	5660	127.9	22.6	5660	32.7	5.8
(b) *Limecola balthica*	Sandy			Muddy		
Treatment	Density	Biomass	Body size	Density	Biomass	Body size
1	0	0	0	0	0	0
2	943	7.1	7.6	943	4.8	5.1
3	943	24.2	25.9	943	16.0	17.0
4	943	29.3	31.4	943	21.1	22.4
5	1868	48.9	26.2	1887	32.7	17.4
6	2802	9.5	3.4	2830	11.8	4.2
7	2802	49.5	17.7	2830	18.9	6.7
8	2802	67.1	23.9	2830	51.4	18.2
9	4670	27.8	6.0	4717	17.6	3.7
10	4670	67.5	14.4	4717	40.3	8.5
11	5604	36.5	6.5	5660	11.2	2.0

575

576   *Table 3*

(a) *Hediste diversicolor*	Type III Sum of Squares	df	Mean Square	F	p-level
Corrected Model	36660.8	2	18330.4	52.8	<0.001
Intercept	4416.7	1	4416.7	12.7	<0.001
Biomass	36228.7	1	36228.7	104.4	<0.001
Sediment type	61.8	1	61.8	0.2	0.678
Error	5897.8	17	346.9		
Total	197874.5	20			
Corrected Total	42558.6	19			
R Squared = 0.86 (Adjusted R^2 = 0.85)					
(b) *Limecola balthica*	Type III Sum of Squares	df	Mean Square	F	p-level
Corrected Model	991.2	2	495.6	50.4	<0.001
Intercept	67.5	1	67.5	6.9	0.018
Biomass	934.4	1	934.4	95.1	<0.001
Sediment type	344.1	1	344.1	35.0	<0.001
Error	167.1	17	9.8		
Total	5886.0	20			
Corrected Total	1158.4	19			
R Squared = 0.86 (Adjusted R^2 = 0.84)					

577

578

579

580

581

582

583

584

585

586

587   *Table 4*

Faunal-mediated O_2 uptake		=a(Bodysize)^{b}Density					=c(Biomass)^d				
Species	Sediment type	a	b	R^2	Adj. R^2	p	c	d	R^2	Adj. R^2	p
Limecola balthica	Sandy	0.10	0.69	0.64	0.6	0.005	1.29	0.65	0.63	0.59	0.006
	Muddy	0.37	0.83	0.88	0.87	<0.001	2.58	0.62	0.93	0.92	<0.001
Hediste diversicolor	Sandy	0.39	0.58	0.75	0.72	0.001	9.75	0.58	0.96	0.95	<0.001
	Muddy	0.90	0.78	0.86	0.85	<0.001	6.25	0.71	0.99	0.98	<0.001

588

589

590

591

592

593

594

595

596

597

598

599

600

601

602

603

604

605

606

607   **Figures**

608   *Figure 1*: Faunal-mediated O_2 uptake (mmol.m^{-2}.d^{-1}) measured in each microcosm as a function of

609   *Hediste* (a) and *Limecola* (b) biomass (gAFDW.m^{-2}). Allometric model fits Y =cW^d (see Table 3) are

610   presented in blue (muddy sediment) and red (sandy sediment).

611   *Figure 2*: Scatterplots of faunal-mediated O_2 uptake (mmol.m^{-2}.d^{-1}) against *Hediste* (a) and *Limecola* (b)

612   – mediated uranine flux (L.m^{-2}.d^{-1}) measured in muddy (blue) and sandy (red) sediments. Linear fits and

613   regression statistics are presented in the figure legend.

614

615

616

617

618

619

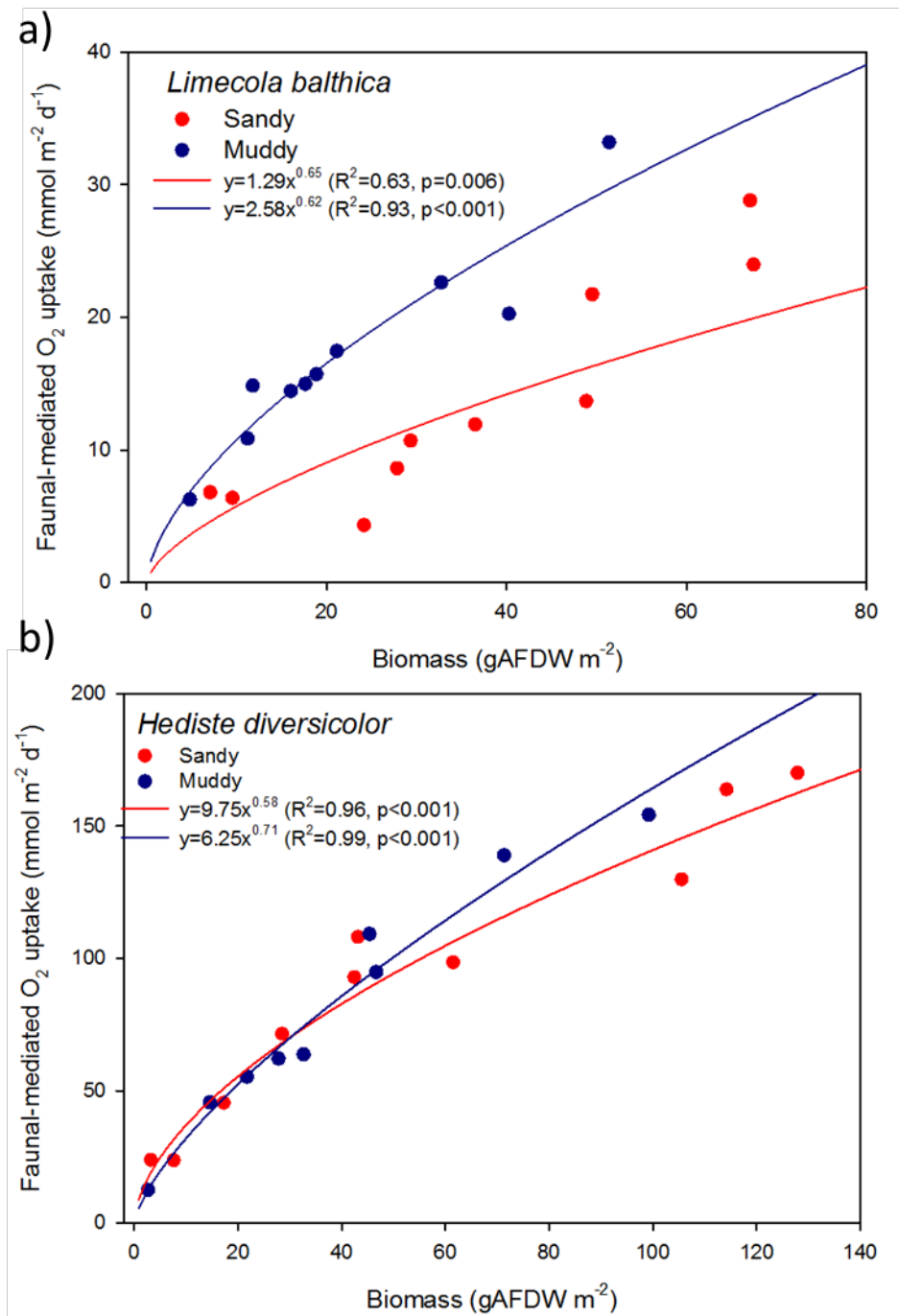620

621

622

623

624

625

626

627

628

629

630

631

632   *Figure 1*

633

634

635

636

637

638

639

Figure 2